Journal of Biomedical Materials Research Part B: Applied Biomaterials

WILEY

Society For Biomaterials

RESEARCH ARTICLE OPEN ACCESS

Soft Scaffolds for Nerve Repair: Investigating Glycerol-Plasticized Chitosan Microstructures With In Vitro Complex Models

Luca Scaccini[1,2] | Enrique Escarda-Castro[3] | Adrián Seijas-Gamardo[3] | Hao Wu[3] | Tomás Santos Coimbra[3] | Stefania Raimondo[4] | Federica Fregnan[4] | Luisa Muratori[4] | Marco Cecchini[2] | Lorenzo Moroni[3] | Paul Wieringa[3] | Ilaria Tonazzini[2]

[1]NEST, Scuola Normale Superiore, Pisa, Italy | [2]Istituto Nanoscienze – CNR, Pisa, Pisa, Italy | [3]MERLN Institute for Technology-Inspired Regenerative Medicine, Maastricht University, Maastricht, ER, the Netherlands | [4]Department of Clinical and Biological Sciences, Neuroscience Institute Cavalieri Ottolenghi (NICO), University of Turin, Orbassano, Turin, Italy

Correspondence: Paul Wieringa (p.wieringa@maastrichtuniversity.nl)

Received: 14 July 2025 | **Revised:** 12 September 2025 | **Accepted:** 19 September 2025

Funding: The authors received no specific funding for this work.

Keywords: chitosan | in vitro | microstructures | nerve model | nerve regeneration | scaffolds

ABSTRACT

Peripheral nerve injuries are a significant clinical concern, often resulting in incomplete functional recovery due to the limitations of current treatments. Biomaterial-based scaffolds that mimic the mechanical and topographical features of native nerve tissue represent a promising strategy to support regeneration. In this study, we investigate the regenerative potential of soft and nerve-mechanically compliant glycerol-plasticized chitosan (Gly–chi) microstructured membranes with in vitro models with increasing biological complexity. These soft directional microgrooved membranes promoted invasion, polarization, and alignment of primary Schwann cells (SCs), and further promoted neurite outgrowth and directional guidance of human iPSC-derived sensory neurons when co-cultured on SCs. Moreover, tests with rat dorsal root ganglia (DRG) explants confirmed the ability of these scaffolds to orient axonal extension also in an ex vivo setting. Interestingly, neurites aligned even over a confluent SC layer, indicating that topographical cues may be transmitted via SC-mediated signaling in addition to direct contact. Overall, our findings demonstrate that glycerol-blended chitosan membranes with a physiological-grade stiffness, similar in respect to nerve tissues, and micro-structured with directional grooves effectively support both glial and neuronal organization and represent a robust biomimetic platform for peripheral nerve repair and advanced in vitro modeling applications.

1 | Introduction

Peripheral nervous injuries (PNIs) are a common issue affecting 13–23 per 100,000 people, leading to long-term painful disability and reduced quality of life [1]. Peripheral nerves have a natural regenerative capability, but in most cases, the healing process is not successful when the damage is serious or extensive [2]. When these conditions occur, autologous transplants, using the patient's own nerves, are still considered the best treatment options, even if they are tied to several flaws, including issues for the donor, a limited supply of graft, and irregular recovery [3]. For this reason, there is a strong need for new ways through bioengineering that can assist and boost nerve repair.

In recent years, nerve guidance conduits (NGCs) have been designed and tested to act as scaffolds and to support an effective

regeneration of peripheral nerves. While some are already in use in clinics, they often fail to outperform the abovementioned traditional surgical methods [4–6].

Several key parameters are important in the design and production of an effective scaffold, such as biodegradability, immunogenicity, and superficial functionalization. In this framework, chitosan, a biocompatible and biodegradable polymer coming from the controlled deacetylation of chitin, is promising and already in use for the creation of NGCs.

We already demonstrated the possibility of using microstructured chitosan membranes to direct the morphology and migration behavior of Schwann cells (SCs) [7], one of the most important cells to participate in the nerve regeneration process [8]. We investigated directional micropatterns with different levels of axial symmetry: gratings (GR; alternating lines of ridges and grooves), a symmetric pattern expected to impose strict alignment; zig-zag patterns of scalene triangles (SCA), an asymmetric geometry known to leave more degrees of freedom to SCs [7]. This guidance is possible thanks to the ability of neural cells to respond to superficial oriented microtopographies and orient themselves accordingly [9–11], making the use of these patterns a new possibility in NGCs.

Mechanical features also play a pivotal role in determining cell fate, and substrate stiffness is emerging as a key regulator of nervous tissue development/regeneration [12, 13]. We further studied the impact of chitosan's stiffness, showing how a combination of directional anisotropic microtopographies and mechanical properties (i.e., soft), more compliant with nerve tissues, can be beneficial for SCs' responses needed in peripheral nerve regeneration [14]. In fact, we observed that SCs' wound healing was sped up on glycerol-plasticized soft chitosan microstructured membranes when compared to pure chitosan membranes, both on GR and SCA geometry. Our results showed how mechanical compliance of substrates is a key parameter when designing nerve scaffolds.

Overall, these microstructured soft scaffolds showed potential for a clinical translation. Progress in scaffold production has not always translated into clinical solutions because of the limitations due to the methods used in laboratories to test them. On one side, traditional two-dimensional (2D) cell culture systems are widely used, despite they often failing to mimic the intricate architecture and complex dynamic environment of the native tissues [15, 16]. On the other side, animal models are complex tools, with high costs and several ethical concerns: the issues related to the 3R's principles and the reduction of animal use in research pose further questions for in vivo tests [17, 18]. For these reasons, in recent years, more advanced in vitro models have been introduced, also thanks to the possibilities opened by the use of induced pluripotent stem cells (iPSCs), in particular in the neuronal field. Today, several three-dimensional (3D) cell models, such as 3D in vitro nerve models, have been developed and tested [19–21], shedding additional light on the possible regenerative scenario of scaffolds and biomaterials.

For instance, Kraus et al. developed a 3D in vitro model with SCs–neuroblastoma spheroids in a collagen matrix, underscoring the value of 3D configurations for studying cell–cell interactions within biomaterial scaffolds [22]. Moreover, Lin et al. used SC-like cells derived by umbilical cord blood mesenchymal stem cells to assemble 3D cell spheroids by using a methylcellulose hydrogel system and found that their transplantation leads to enhanced functional recovery after sciatic nerve injury in vivo [23]. In another study by Haycock et al., a 3D in vitro peripheral nerve model was created using aligned electrospun polycaprolactone fiber scaffolds, demonstrating that both neurite outgrowth and SCs migration are influenced by fiber diameter and that co-cultures induce aligned neurite guidance and SC co-localization [24]. Furthermore, we have also developed a sensory nerve model in vitro, using induced pluripotent stem cells–derived nociceptors (that are electrically active and exhibit a functional response to noxious stimuli), co-cultured with primary SCs on an aligned microfibrous scaffold [25].

Such models that combine neurons and Schwann cells as well as other cell types are becoming increasingly important for evaluating scaffolds for neural applications. The use of such models allows mechanistic examinations of how axons navigate more physiologically representative 3D environments and permits the study of myelination and repair mechanisms. Advanced in vitro nerve models are therefore a fundamental next step for testing biomaterials and scaffolds for PNIs before their clinical translation.

In this research, we generated glycerol-chitosan plasticized (Gly-Chi) soft scaffolds with microstructured directional topographies, GR and SCA. We tested them with increasingly complex in vitro systems: dorsal root ganglia (DRGs) explants and an in vitro sensory nerve model made of primary SCs and sensory neurons derived from human iPSCs in order to assess their performances in a more in vivo-*like* condition.

2 | Materials and Methods

2.1 | Production of Glycerol-Blended Chitosan Membranes

10% glycerol blended microstructured chitosan membranes were obtained through a two-step solvent casting procedure, as described in Scaccini et al. [14]. Briefly, microstructured silicon wafers, presenting directional microtopographies, were developed through the photolithography technique and used as primary molds to create PDMS intermediate molds through replica molding. The glycerol-plasticized chitosan (Gly-Chi) solution was obtained by dissolving 2% by weight chitosan powder (Sigma–Aldrich, 448877) in an acetic acid solution (1% v/v in deionized water). Then, it was stirred overnight at RT and filtered using a Buchner funnel and filter paper with a 10 μm cutoff (Superfiltro, Milano). The solution was then directly poured over the PDMS intermediate mold. The membranes were dried under a chemical hood for 72 h and detached using forceps. The Gly-Chi membranes were further neutralized using a NaOH solution of 125 mM for 30 min and washed twice using DI water.

We produced the following directional micro-patterns, both with a period (ridge + groove width) of ≈10 μm and a depth of 1.3 ± 0.1 μm, presenting different levels of symmetricity: gratings (GR), with alternating lines of grooves and ridges, and with

two symmetry axes (i.e., higher symmetry); zig-zag pattern with scalene triangles (SCA), and with one symmetry axis (i.e., lower symmetry), as in [14]. Flat molds were used to produce FLAT isotropic membranes, as a control condition. Before cell testing, the neutralized membranes were treated with a solution of ethanol 70% V/V and washed three times with DI water.

2.2 | Rat DRG Dissection and Organotypic Cultures

Rat dorsal root ganglia (DRG) dissociated neurons and explants were used to study neurite outgrowth on membranes [26].

DRGs were obtained from adult female Wistar rats (approximately 250 g body weight, Envigo, Udine, Italy). Animals were housed under controlled environmental conditions (temperature, humidity, 12-h light/dark cycle) with free access to food and water. All procedures complied with EU Directive 2010/63 and were approved by the University of Turin Ethical Committee (Ministry of Health project no. 583/2020). The harvesting of DRGs for sensory neuron dissociation and organotypic cultures has been previously described [27]. After harvesting, DRG neurons were dissociated following the protocol previously described [28]. They were seeded on the different micro-grooved substrates pre-coated with laminin (2 μg/cm^2, Sigma) in 24-well culture dishes and cultured as in [28].

For DRG explant cultures, the connective tissue capsule around the ganglia was removed and each ganglion was cut in half to aid the attachment on the substrate. Explants were seeded in a 50 μL drop of Geltrex (ThermoFisher) in F12 medium (50% v/v) and after 2 h of incubation at 37°C, serum-free culture medium (SFM) with nerve growth factor (NGF, 50 ng/mL, Invitrogen) was slowly added to the plate, as in [29]. Briefly, SFM medium is composed of 50% (v/v) F12 nutrient mixture, 50% (v/v) basal medium Eagle (BME), 2×10^{-3} M glutamine, 0.5% (v/v) 100× PSN antibiotic mixture (all from ThermoFisher-Invitrogen), 10 mg/mL bovine albumin serum, 1×10^{-4} M putrescine, 0.1 mg/mL transferrin, 3×10^{-8} selenium, 0.005 mg/mL insulin, 3.8×10^{-5} M vitamin C, 7.5 mg/mL glucose (all from Sigma–Aldrich) in culture-grade water. After 3 days of culture, organotypic ganglia and DRG dissociated neuronal cultures were fixed in 4% paraformaldehyde for 15 min, washed in 0.1 M phosphate buffer (PBS, pH 7.2), and processed for immunostaining.

We analyzed $n=8$, 8, and 14 DRG dissociated neurons on Flat, GR, and SCA, respectively; we analyzed $n=8$ and 5 explants on GR and SCA, respectively.

2.3 | Primary Schwann Cells Harvesting, Purification and Culture

Primary SCs were harvested from the sciatic nerves of neonatal (P1–P3) Wistar rat pups (both males and females), following protocols compliant with the Dutch Animal Experimental Act and approved by the local ethical committee and Dutch national ethical authority (license registration number 10700). The extraction and digestion of nerve segments and SCs isolation and purification were conducted as previously described by [30] and originally reported by Kaewkhaw et al. [31]. Peripheral nerves were minced and enzymatically digested in 0.05% (w/v) collagenase for 60 min at 37°C under 5% CO_2. The resulting cell suspension was passed through a 40 μm strainer, centrifuged at 400 g for 6 min, and the supernatant discarded. The pellet was washed with DMEM supplemented with 10% fetal bovine serum (FBS), 100 U/mL penicillin, and 100 μg/mL streptomycin, then centrifuged again under the same conditions. Cells were finally resuspended in 2 mL of Schwann cell culture medium containing DMEM, D-valine (Cell Culture Technologies), 2 mM L-glutamine, 10% (v/v) FBS, 1% (v/v) N2 supplement (R&D Systems), 20 μg/mL bovine pituitary extract, 5 μM forskolin, 100 U/mL penicillin, 100 μg/mL streptomycin, and 0.25 μg/mL amphotericin B (all Sigma–Aldrich). Cell suspensions were plated onto 35 mm Petri dishes pre-coated with 1 μg/mL laminin (R&D Systems) and maintained at 37°C, 5% CO_2. The inclusion of D-valine, instead of L-valine, selectively inhibited fibroblast proliferation while supporting Schwann cell survival and growth. After 7 days, 1 mL of fresh medium was added, followed by medium changes every 2 days until cultures reached confluency. Cells between passages 3 and 8 (P3–P8) were used for experiments.

2.4 | IPSCs-Derived Sensory Neurons Production

Induced pluripotent stem cells (iPSCs)-derived *sensory neurons* (i.e., specialized peripheral sensory neurons) were obtained through a multi-step differentiation protocol, as described in [25]. Briefly, the human iPSC line LUMC0031iCTRL08 (provided by the Leids Universitair Medisch Centrum iPSC core facility) was cultured on Geltrex-coated dishes at a density of 10×10^3/cm^2 in mTeSR Plus medium (Stem Cell Technologies). Cells were fed every day with completely fresh medium and passaged weekly using Gentle Cell Dissociation Reagent (Stemcell Technologies).

To induce iPSCs differentiation into *sensory* neurons (SNs), cells were detached with Accutase and seeded in custom-made agarose microwells, using mTeSR Plus medium supplemented with 10 μm of Y-27-632 and 0.5% Geltrex (in solution); cell synchronization was initiated by the addition of mTeSR Plus medium supplemented with 1% dimethyl sulfoxide (DMSO). Cell differentiation was initiated by the addition of dual mothers against decapentaplegic (SMAD) inhibition media, containing Advanced RPMI 1640 supplemented with Glutamax (both ThermoFisher Scientific), 100 nM LDN-193189 (Tocris), and 10 μM SB431542 (Tocris). The spheroids were maintained for 48 h in the dual SMAD inhibition medium. Following this, SNs commitment was induced via media containing Advanced RPMI 1640 supplemented with Glutamax, 3 μM CHIR99021 (Tocris), and 1 μM retinoic acid (Tocris). The spheres were maintained in the SN induction media for 5 days, with media change every alternate day. Following this stage, the spheres were incubated in notch inhibition media, consisting of Advanced RPMI supplemented with Glutamax, 10 μM SU5402 (Tocris), and 10 μM (2S)-è*N*-[(3,5-Difluorophenyl)acetyl]-L-alanyl-2-phenylglycine 1,1-dimethylethyl ester (DAPT) (Tocris), for 48 h.

Finally, the neurospheres, composed of immature SNs cells, were collected and seeded on Gly-Chi microstructured membranes. Here, SNs were cultured in neural maturation medium for 7 days, to reach the full sensory neuron phenotype. (see later

for details) The neural medium is composed of Neurobasal Medium, 0.5 mM Glutamax, 100 U/mL penicillin and 100 μg/mL streptomycin (all ThermoFisher Scientific), 100 ng/mL human nerve growth factor (NGF), 50 μg/mL ascorbic acid (all Sigma–Aldrich), 25 ng/mL human neuregulin-1 type III (NRG-1), sensory and motor neuron-derived factor (SMDF) and N21 supplement (both from R&D systems).

2.5 | Peripheral Nerve Model

In order to test the in vitro peripheral nerve model, primary SCs and SNs were co-cultivated over the Gly-Chi microstructured membranes. Firstly, primary SCs were seeded over laminin-coated Gly-Chi membranes (1 μg/mL Laminin-1, R&D systems, and 2 μg/mL Poly-D-Lysine, Sigma–Aldrich, solution in PBS, incubated overnight at 37°C [30]), at a seeding density of 30,000 cells/cm^2. SCs were let grow for 7 days, changing the media every other day. After this time, spheroids were seeded on the top, and culture media was replaced with SNs specific media. Spheroids were mechanically detached from the collagen microwells, pipetting up and down. Then, spheroids were collected in a tube and seeded one by one, using a cut p200 serological pipette tip, over the Gly-Chi microstructured membranes. The SNs spheroids were let grow for 7 days, changing the media every 2 days.

As control, SNs-only cultures were produced using the same protocol, but directly putting the SN spheroids over laminin-coated Gly-Chi membranes (without SCs layer) and letting them grow for 7 days.

Eventually, after 7 days for primary SC cultures and SN-only cultures and 7 + 7 days for primary SC-SN co-cultures, samples were fixed for 30 min using a 4% paraformaldehyde (PFA) solution, and stocked at 4°C for further immunostaining. We analyzed $n = 7$, 17, and 13 SCs + SNs on Flat, GR, and SCA respectively, while $n = 4$, 12, and 4 SNs on Flat, GR, and SCA, respectively.

2.6 | Immunocytochemistry

Fixed samples were permeabilized for 30 min at RT with 0.1% Triton X-100 in PBS, followed by rinsing with PBS and blocking with blocking buffer (5% goat serum, 0.05% Tween-20, and 1% BSA in PBS) overnight at 4°C under mild agitation. After that, samples were incubated overnight at 4°C with primary antibodies in blocking buffer. For SCs, primary antibodies were: c-Jun (Cell Signaling, #9165 1:300, rabbit) and S100 (Sigma–Aldrich, S2644, 1:500, mouse). For SNs, primary antibodies were: anti-βIII-tubulin (Novus Biologicals, NB100-1612, 1:1000, chicken); anti-myelin-binding-protein (anti-MBP, Invitrogen, PA1-46447, 1:100, rabbit). The next day, samples were washed with blocking buffer and incubated overnight at 4°C with secondary antibody solutions in blocking buffer. Secondary antibodies were: goat anti-rabbit Alexa Fluor 750 (Invitrogen, A-21039, 1:500), goat anti-mouse 647 (Invitrogen, A-21039, 1:500), and goat anti-chicken Alexa Fluor 647 (Invitrogen, A-21449, 1:500). The day after, samples were washed with PBS, incubated with Alexa Fluor 488 Phalloidin (Invitrogen, A12379, 1:50), and washed again with PBS.

2.7 | Imaging and Image Analysis

Samples were imaged using a Nikon Eclipse Ti inverted epifluorescence microscope. Each reported image was obtained from a z-series. The resulting images were obtained by processing each channel with ImageJ software (NIH), using the Extended Depth of Field plugin (developed at EPFL, Switzerland).

Cell cytoskeleton organization was quantified by analyzing the actin fibers (for SCs) or βIII-tubulin (for neurons) fluorescence signal with the "Directionality" tool in FIJI (http://fiji.sc/Fiji), similarly as before [7]. This plugin returns a directionality histogram by exploiting image fast Fourier transform (FFT) algorithms: isotropic images generate a flat histogram, whereas oriented images give a peaked histogram. These histograms are fitted by Gaussian curves that return two parameters, dispersion and directionality (the standard deviation and the center of the Gaussian curve, respectively), the first representing the degree of orientation of the image, and the second representing the direction in which it is oriented (here normalized to the underlying pattern orientation direction); the image dimension was kept fixed to $187 \times 187\,\mu m^2$, and we analyzed at least five fields/sample.

c-Jun expression was evaluated by tracking a ROI around each nucleus and measuring the mean fluorescence in the c-Jun channel. We considered positive the cells having a mean intensity fluorescence signal that was 80% higher than the measured signal of the background; we analyzed at least 200 nuclei/sample.

Neurites coming from the SNs spheroids were tracked with ImageJ software, using the NeuronJ plugin. The length and angle of neurites were determined by processing the neurite tracings, using a custom-made MatLab (MathWorks, MA, USA) script, as in [32].

2.8 | Statistical Analysis

Data are reported as the average value ± the standard deviation (mean ± SD). One-way ANOVA (Bonferroni multiple comparison test) was used to compare different conditions, if not stated differently. For selected experiments, two-way ANOVA analysis or Student's *t*-test (unpaired) was used to compare different groups or two conditions, respectively. Statistical significance refers to results where $p < 0.05$ was obtained.

3 | Results

3.1 | In Vitro and Ex Vivo DRG Neuronal Models on Gly-Chi Membranes

We initially tested our micro-patterned membranes with both in vitro and ex vivo rat neuronal models, studying their interaction with rat DRG dissociated neurons and organotypic cultures of DRG explants.

The culture of both dissociated DRG neurons (Figure 1a) and DRG explants (Figure 1b,c) on GR and SCA glycerol-chitosan substrates grew up to 3 days and demonstrated orienting the development of neurites along both micropatterns. For rat dissociated DRG

neurons, neurites presented a mean directionality of 4.1° ± 5.9° on GR and 5.0° ± 3.7° on SCA, and a dispersion of 4.8° ± 4.3° on GR and 9.2° ± 3.9° on SCA ($p < 0.05$ GR vs. SCA, Student *t*-test; mean ± SD). As a control condition, we report that DRG dissociated neurons on flat chitosan substrates present a random directionality of 42.0° ± 18.0° and a dispersion of 14.1° ± 5.7°. Moreover, both GRs and SCA anisotropic patterns were highly efficient in directing DRG explant neurites (Figure 1b,c), resulting in a mean directionality of 5.5° ± 7.9° on GR and 5.8° ± 4.1° on SCA (with respect to pattern main direction), while the dispersion of neurite fibers was 5.0° ± 2.2° on GR and raised up to 14.9° ± 5.9° on SCA ($p < 0.001$ GR vs. SCA, Student *t*-test; mean ± SD). Taken together, these results indicate that: GR and SCA topographies are able to align and direct both dissociated DRG neurons and ex vivo ganglia explants; the anisotropic and more asymmetric pattern SCA leaves a higher degree of freedom to DRG and ganglia neurites' organization, as shown by the higher dispersion values of cytoskeleton signal.

3.2 | Effect of Gly-Chi Microstructured Substrates on Primary SC Morphology, Polarization, and c-Jun Expression

Gly-Chi microstructured membranes were cultured with primary SCs and tested for their ability to sustain primary SC growth and direct/improve their polarization and migration. As expected, Gly-Chi membranes showed the ability to properly support cell growth and confluency. We analyzed the morphology of primary SCs cultured on our films by immunostaining (Figure 2). An immunostaining against S100 was performed (Figure 2a), confirming the general purity of the cultures used. Following this, an actin staining revealed the organization of the cytoskeleton in primary SC layers grown on Gly-Chi microstructured membranes. Actin filaments were assessed by Fast Fourier Transform (FFT) analysis of the fluorescent images, providing measurements of actin directionality and dispersion and metrics of orientation and degree of alignment, respectively (Figure 2b,c). As expected, both the GRs and SCA anisotropic patterns were highly efficient in orienting SC actin fibers (GR = 2.4° ± 1.8° and SCA = 3.6° ± 2.6°, $p < 0.001$ GR/SCA vs. FLAT), while on the FLAT, cells were randomly oriented (average angle ≈ 45°; Figure 2b); and in polarizing the fibers along the pattern by significantly decreasing the dispersion of the actin signal (GR = 11.2° ± 2.8° and SCA = 12.0° ± 2.7°, $p < 0.001$, FLAT vs. GR and $p < 0.01$ FLAT vs. SCA; Figure 2c). Finally, we investigated the expression of c-Jun, which is a specific SC marker for their proliferating phenotype and is known to be activated in case of PNI (i.e., during SCs' phenotypic switch from myelinating to repairing phenotype). c-Jun expression resulted similar in all the patterns (Figure 2d).

Overall, Gly-Chi microstructured membranes were shown to support the growth of primary SCs and to well orient their cytoskeleton toward the direction of both directional patterns.

3.3 | In Vitro Sensory Nerve Model on Gly-Chi Membranes

Finally, we proceeded with the addition of IPSCs-derived sensory neurons onto membranes seeded with SCs, to test the entire

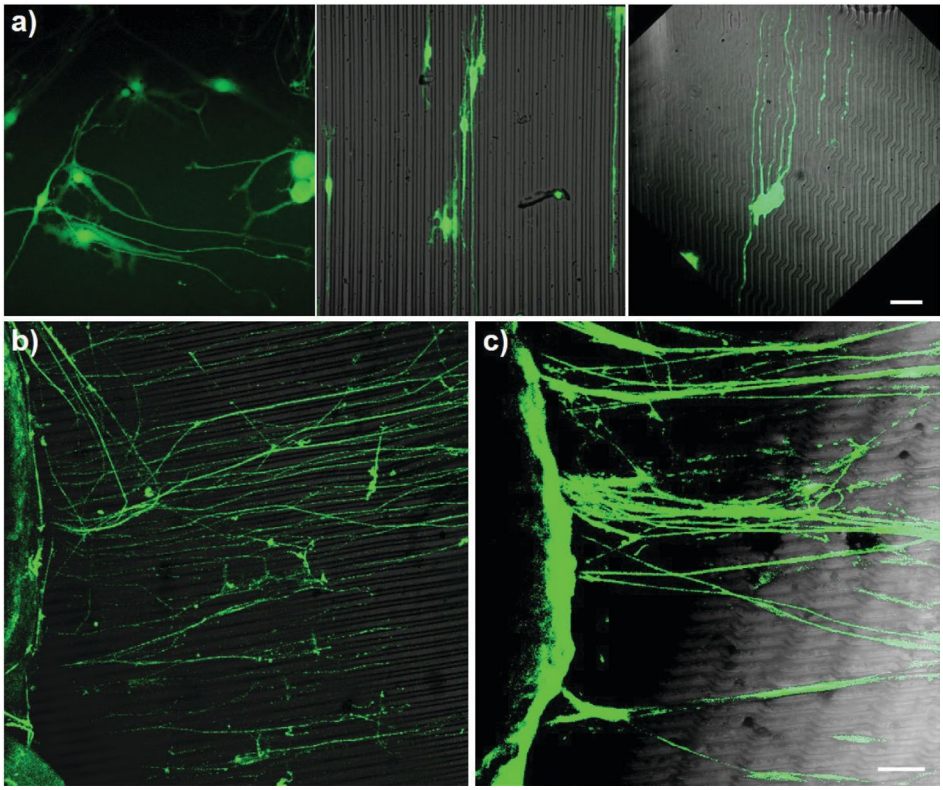

FIGURE 1 | (a) Representative images of rat dissociated DRG neurons cultured on FLAT (left), GR (center), SCA (right) chi membranes; (b, c) representative images of DRG explant cultures on GR (b) and SCA (c) topographies with zoom on their neurites network. Immunostaining for βIII-tubulin (in green); scale bars = 100 μm.

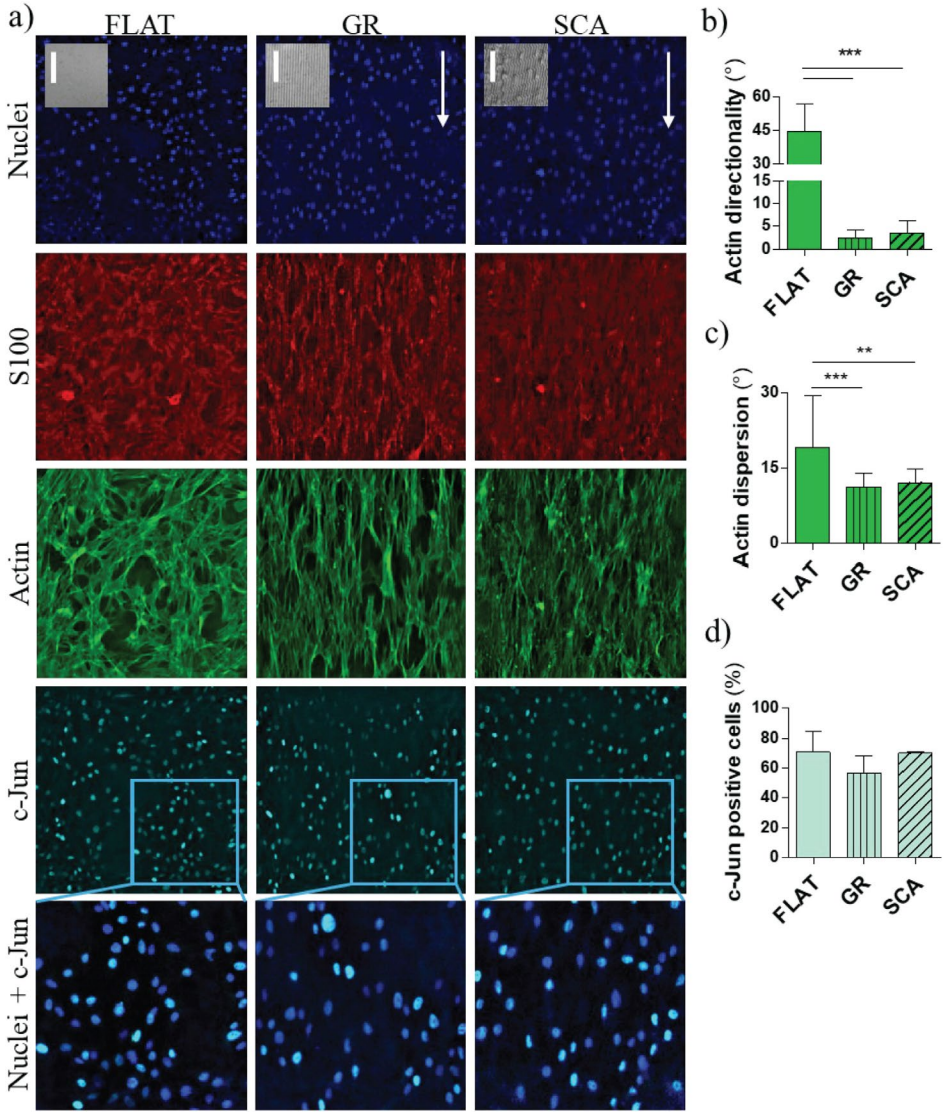

FIGURE 2 | Primary Schwann cell morphological analysis and c-Jun expression analysis. (a) Fluorescent images of primary SCs cultured on FLAT, GR and SCA Gly-chi membranes: from left to right, nuclei (blue), with patterns' bright field inserts, S100 (red) actin fibers (green), and c-Jun (cyan); scale bar = 100 μm. (b, c) Actin organization analysis: (b) actin directionality and (c) actin signal dispersion. (d) percentage of c-Jun positive nuclei. */***$p < 0.05/0.001$, One-way ANOVA with Bonferroni's test. Data = mean ± SD.

in vitro nerve sensory model. As a control condition, we also cultured SNs on membranes in the absence of primary SCs. A scheme illustrating the composition of the in vitro nerve model can be seen in Figure 3a. Our qualitative observations revealed that soft Gly-Chi membranes allowed the growth of SCs-SNs co-cultures. After 7 days, SN neurites were present, both in the presence and absence of primary SCs (Figure 3b). SN neurites cultivated over GR/SCA Gly-Chi membranes exhibited a bipolar distribution, with axons mainly present at the sides of the SN spheroids oriented along the pattern direction. Conversely, neurites from SN spheroids cultivated on FLAT substrates had an isotropic distribution, growing all around the neurosphere (Figure 3b).

Quantifying the alignment of SNs neurites revealed that GR and SCA membranes were able to significantly align neurites along the main direction of their pattern, both in the presence (GR = 6.9° ± 2.1° and SCA = 6.3° ± 6.4°, $p < 0.01/0.001$ FLAT vs. SCA and vs. GR; Figure 3c-right panel) and absence of the underlying SCs layer (GR = 7.3° ± 3.2° and SCA = 5.9° ± 4.8°, $p < 0.001$ FLAT vs. GR and vs. SCA, Figure 3c-left panel). Importantly, SCs were able to transduce the topographical signal from the GR/SCA topography to SNs, similarly to the effect of direct contact guidance of the substrates on SNs.

In addition, the presence of SCs led to a significant enhancement in the neurite length of SNs ($p < 0.001$, SCs + SNs vs. SNs, Two-Way ANOVA, Figure 3d). The average neurites' length of SNs cultured on SCs was further boosted on microstructured Gly-Chi substrates: here, in particular, neurites of SC + SNs cultured on GR showed an average length of 748 ± 177 μm against an average value on FLAT substrates of 510 ± 122 μm ($p < 0.05$ FLAT vs. GR; Figure 3d-right). A morphological assessment of the SN spheroids also found that co-cultures (SCs + SNs) generated slightly bigger neurospheres ($p < 0.001$ SCs + SNs vs. SNs, Two-Way ANOVA; Figure 3e), even if they did not show any polarization along the patterns.

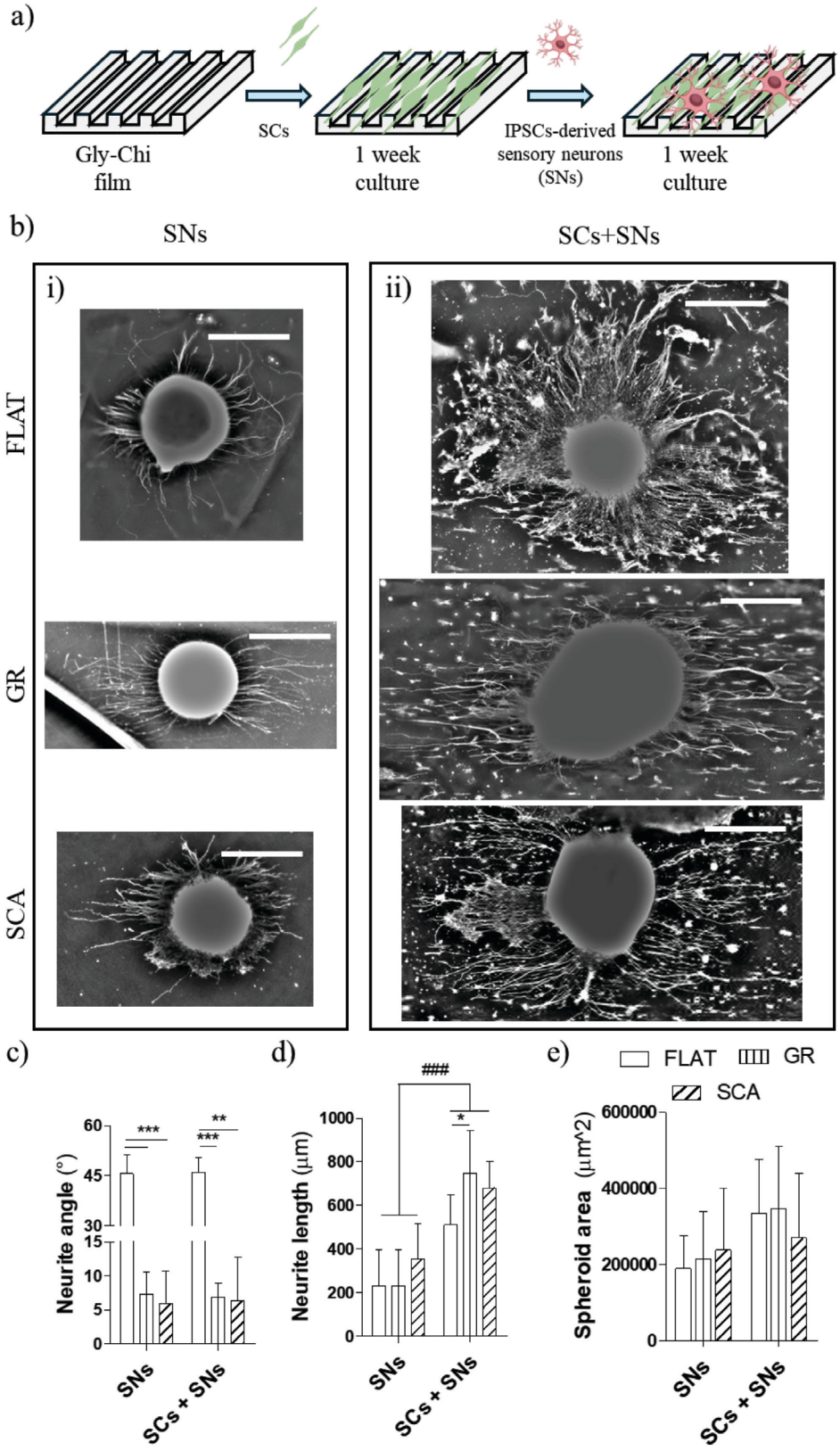

FIGURE 3 | Characterization of sensory neurons morphology on microstructured Gly-chi membranes, in presence or absence of primary SCs, after 7 days of culture. (a) Immunostaining to βIII-tubulin showing the overall axonal growth in presence (left column) or absence (right column) of primary SCs, on Flat, GR and SCA membranes. Scale bar = 500 μm. (c, d) Quantification of (c) neurite length (in μm), and (d) neurite angle of alignment for SNs and SCs + SNs; */** $p < 0.05/0.01$, One-way ANOVA with Bonferroni's test. Data = mean ± SD. (e) Quantification of neuronal spheroid somas' area (in μm^2), in the different culture conditions; ### $p < 0.001$, Two-way ANOVA test. Data = mean ± SD.

By merging the fluorescent signals of SNs (stained by βIII-tubulin) and SCs (stained by actin fibers) (Figure 4a), it is possible to visualize well visualize the alignment of both the elements. In particular, the presence of a layer of aligned primary SCs over the microstructured Gly-Chi membranes induces the alignment of the neurites growing over them, thus mimicking the exact in vivo process of nerve regeneration. We also analyzed the SNs networks by FFT directionality. In agreement with previous data, both the GRs and SCA patterns were efficient in directing neurites also when growing on the SC's layer (GR = 3.9° ± 2.1° and SCA = 7.5° ± 7.1°, $p < 0.001$ GR/SCA vs. FLAT; Figure 4b). The dispersion of the tubulin signal is instead similar in all substrates (GR = 12.2° ± 5.2° and SCA = 12.9° ± 6.2°; Figure 4c). Here the directionality and dispersion values of SNs recall the ones obtained by actin fibers' FFT analysis of SCs pure cultures (Figure 2b,c). Separated assessment of SCs' organization from the SCs + SNs cultures in the nerve model reveals that SCs have the same directionality and dispersion values as those for SCs cultured alone.

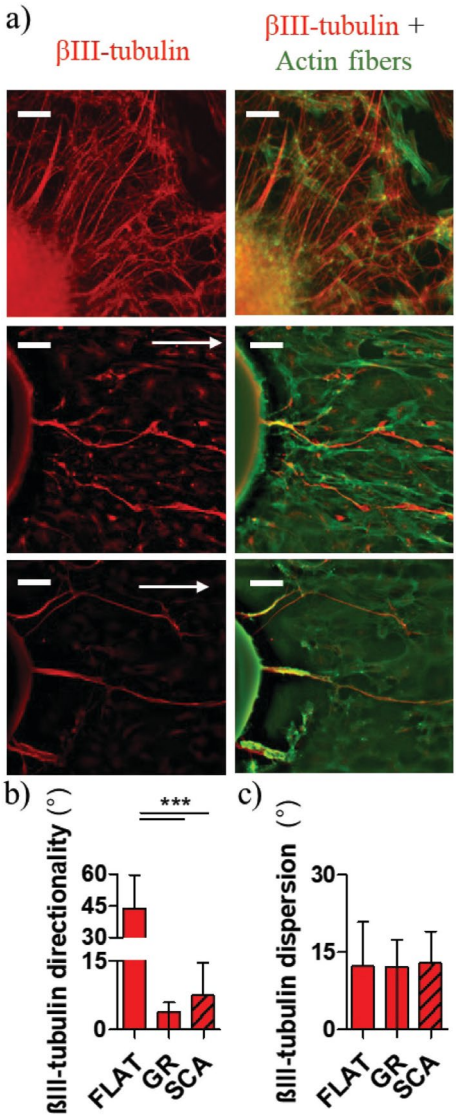

FIGURE 4 | In vitro sensory nerve model on microstructured Gly-chi membranes. (a) Merged channels of representative fluorescent images of in vitro sensory nerve model cultured on flat, GR and SCA Gly-chi membranes: SNs neurites (βIII-tub positive, in red), and SCs (actin-positive, in green); scale bars = 100 μm. (b, c) βIII-tubulin organization analysis, for SNs growing on SCs in the in vitro nerve model: SNs' (b) directionality and (c) dispersion. ***$p < 0.001$, One-way ANOVA with Bonferroni's test. Data = mean ± SD.

Overall, the in vitro nerve model composed by SCs + SNs responded well to GR and SCA Gly-Chi membranes, suggesting that these scaffolds can fully sustain both SCs and SNs growth and polarization. SCs and SNs align accordingly to both GR and SCA topographies, with no main differences related to their different level of axial symmetry. Overall GR scaffolds resulted particularly efficient in elongating neurites' growth.

4 | Discussion

In this work, we tested soft and nerve-mechanically compliant glycerol-chitosan membranes, microstructured with directional cues at different levels of axial symmetry, with increasingly complex in vitro nerve systems, to test their ability to sustain peripheral nerve regeneration. We developed glycerol-blended chitosan GR and SCA membranes with a physiological-grade Young's modulus (≈0.7 MPa), similar in respect to soft nerve tissues (Young's modulus≈0.5 MPa [33]), aiming to improve the mechanical compliance between scaffolds and the peripheral nerve and providing directional cues to the regenerating glial and neuronal cells in a synergic approach.

We started with rat DRG models that showed the biocompatibility and orientation capability of our microstructured membranes. Both GR and SCA tuned the development of ganglion neuritic networks, thus directing them along the patterns. Here SCA, the directional and more asymmetric pattern, seems to leave more freedom to neurites organization (i.e., as shown by the increased dispersion of the neurites' fluorescent signal on SCA), both for dissociated neurons and explants, and similarly to our previous results with single RT4-SCs [7, 14]. However, it is important to note that this model lacks of Schwann cells, making it less suitable to fully replicate the dynamic cellular environment of nerve repair in vivo. This limitation motivated us to move toward more complex in vitro systems by incorporating primary SCs and subsequently co-culturing them with iPSC-derived sensory neurons to better emulate the peripheral nerve injury repair scenario. Therefore, we tested an in vitro nerve sensory model [25], composed of a co-culture of primary SCs and iPSCs derived sensory neurons. We could observe that both glial and sensory neuronal components were able to grow and proliferate over the Gly-Chi membranes and, both singularly and together, sensed the directionality of the micropatterns and aligned accordingly. This was expected for primary SCs, which we sourced from rats. Human SCs were not used due to the lack of reliable protocols for deriving mature, functional cells in vitro, as highlighted by Hoke et al. [34]. Isolating primary human SCs also presents ethical and practical difficulties. Rat SCs remain a valid alternative, as prior studies, including ours, have shown they interact appropriately with human neurons, supporting growth and myelination [25]. Extensive testing was previously performed with the RT4-SCs line, thus optimizing the micropatterns and demonstrating how these microstructured substrates can tune the actin cytoskeleton or cell alignment and migration [14]. Moreover, the level of a marker molecule typical of an SCs

repair phenotype, c-Jun, was constant in all the different geometries. Previous studies have analyzed the expression of genes linked to nervous system regeneration, such as c-Jun, in in vivo models of nerve regeneration, and it is important it remains stable in respect to control groups [28]. c-Jun is a critical transcription factor that enables SCs to adopt a regenerative phenotype after nerve injury: it drives the expression of genes involved in axon guidance, neurotrophic support, and extracellular matrix remodeling, all essential for nerve regeneration. So c-Jun consistent expression suggests that our microstructured membranes support the repair-capable state of SCs without interfering with their regenerative function [35].

With regards to the effect of our membranes on neurons' behavior, we observed here that the dimensionality of our GR and SCA microstructures is adequate to properly guide sensory axons, aligning them and inducing their elongation. Among the patterns, GR demonstrated inducing the growth of the longest SNs neurites, especially in the presence of SCs: this is in good agreement also with another work in which this in vitro nerve model was used [25].

Following PNI, SCs represent one of the major and most essential cellular players in the regenerative process, even if coadjuvated by fibroblasts, perineurial, and inflammatory cells. After injury, myelinating SCs undergo dedifferentiation, temporarily losing their specialized phenotype and adopting a more immature and highly plastic state. SCs begin to proliferate and migrate toward the distal stump of the damaged nerve, where they serve as guides for regenerating axons: their activity helps to establish a regenerative environment by releasing neurotrophic factors, clearing cellular debris, and forming aligned structures (Bands of Bungner) over which axons grow, following their topographical cues [8, 36]. When conduits are implanted, something similar happens [37]. Therefore, it was of our interest to study the interaction between SCs and neurons over our microstructures and, importantly, to understand if the geometrical signal they provide can be sensed by neurons in the presence of SCs. This was confirmed in our experiments: even in the presence of a SCs layer underneath the SN spheroid, neurites sensed the topographical stimuli of the scaffolds and oriented accordingly. In fact, the data obtained by the analysis of SCs and SNs, alone and in co-culture, show matching values, thus suggesting a matching cytoskeleton organization. This process is mainly favored by SCs-mediated transduction of the topographical directionality, in agreement with other in vitro studies. In a work by Georgiou et al., a self-aligned collagen-SCs matrix promoted DRGs neurite extension and alignment, demonstrating how aligned SCs promote the alignment of neuronal axons in the same direction [38]. SCs + SNs align accordingly to both GR and SCA topographies, with no main differences related to their different levels of axial symmetry. In line with our previous finding, the impact of the substrate's axial symmetry on SNs is reduced in softer substrates, such as our Gly-Chi ones [14]. However, GR substrates resulted particularly efficient in boosting neurites' elongation.

In summary, our Gly-Chi microstructured soft membranes are able to efficiently guide also complex nerve systems, ex vivo DRG explants and an in vitro sensory nerve model. Both GR and SCA Gly-Chi plasticized scaffolds effectively sustain glial and neuronal colonization, direct and organize the axonal elongation of sensory neurons, also in presence of a layer of SCs, thus leading to an aligned growth of the neurites in the direction of patterns.

5 | Conclusion

In conclusion, our study demonstrates that glycerol-plasticized chitosan (Gly-Chi) microstructured membranes with directional topographies effectively support the growth, alignment, and interaction of both Schwann cells and iPSC-derived sensory neurons in advanced in vitro models of peripheral nerve regeneration. These scaffolds not only provide synergistic mechanical compliance and topographical signals to glial and neuronal organization, but also enable the transmission of alignment signals through Schwann cells even in co-culture systems. The GR and SCA micropatterns promoted axonal alignment and elongation, and in particular, GR enhanced neurite outgrowth in the presence of Schwann cells. Altogether, our findings highlight the translational potential of Gly-Chi soft scaffolds as biomimetic platforms for peripheral nerve repair strategies and as reliable tools for high-content in vitro modeling of nerve injury and regeneration. These substrates have potential for further applications in the field of nerve regeneration.

Acknowledgments

This work was supported by the project PRIN 2022—2022ZH5M72 (PE11)—ENGInerve—"Development of nano/micro-engineered devices for applications in peripheral nervous system pathological models," financed by PNRR Missione 4—Componente 2—Investimento 1.1 "Fondo per il Programma Nazionale di Ricerca e Progetti di Rilevante Interesse Nazionale (PRIN)," European Union—Next Generation EU. Additional support was provided by the European Research Council under the ERC Stg Project OviChip, grant number 101043014.

Conflicts of Interest

The authors declare no conflicts of interest.

Data Availability Statement

The data that support the findings of this study are openly available in Zenodo at https://zenodo.org/, reference number https://doi.org/10.5281/zenodo.17106639.

References

1. C. A. Taylor, D. Braza, J. B. Rice, and T. Dillingham, "The Incidence of Peripheral Nerve Injury in Extremity Trauma," *American Journal of Physical Medicine & Rehabilitation* 87, no. 5 (2008): 381–385.

2. A. Grosu-Bularda, C. V. Vancea, F. V. Hodea, et al., "Optimizing Peripheral Nerve Regeneration: Surgical Techniques, Biomolecular and Regenerative Strategies-A Narrative Review," *International Journal of Molecular Sciences* 26, no. 8 (2025): 3895.

3. F. Fregnan, L. Muratori, M. El Soury, et al., "Improving Regenerative Capabilities of Peripheral Nervous Cells With Chitosan Microstructured and Functionalized Membranes," *Italian Journal of Anatomy and Embryology* 127 (2023): 119.

4. F. Mankavi, R. Ibrahim, and H. Wang, "Advances in Biomimetic Nerve Guidance Conduits for Peripheral Nerve Regeneration," *Nanomaterials (Basel)* 13, no. 18 (2023): 2528.

5. S. Lee, M. Patel, and R. Patel, "Electrospun Nanofiber Nerve Guidance Conduits for Peripheral Nerve Regeneration: A Review," *European Polymer Journal* 181 (2022): 111663.

6. L. D. Johnson, M. Aleemardani, S. Atkins, F. M. Boissonade, and F. Claeyssens, "Emulsion Templated Composites: Porous Nerve Guidance Conduits for Peripheral Nerve Regeneration," *Materials & Design* 239 (2024): 112779.

7. L. Scaccini, R. Mezzena, A. de Masi, et al., "Chitosan Micro-Grooved Membranes With Increased Asymmetry for the Improvement of the Schwann Cell Response in Nerve Regeneration," *International Journal of Molecular Sciences* 22, no. 15 (2021): 7901.

8. R. Deumens, A. Bozkurt, M. F. Meek, et al., "Repairing Injured Peripheral Nerves: Bridging the Gap," *Progress in Neurobiology* 92, no. 3 (2010): 245–276.

9. I. Tonazzini and M. Cecchini, "Neuronal Mechanisms for Nanotopography Sensing," *Frontiers in Nanomedicine Nanomedicine and Neurosciences: Advantages, Limitations and Safety Aspects* 2 (2017): 101–114.

10. I. Tonazzini, E. Jacchetti, S. Meucci, F. Beltram, and M. Cecchini, "Schwann Cell Contact Guidance Versus Boundary -Interaction in Functional Wound Healing Along Nano and Microstructured Membranes," *Advanced Healthcare Materials* 4, no. 12 (2015): 1849–1860.

11. A. Ferrari, M. Cecchini, A. Dhawan, et al., "Nanotopographic Control of Neuronal Polarity," *Nano Letters* 11, no. 2 (2011): 505–511.

12. D. E. Koser, A. J. Thompson, S. K. Foster, et al., "Mechanosensing Is Critical for Axon Growth in the Developing Brain," *Nature Neuroscience* 19, no. 12 (2016): 1592–1598.

13. E. H. Barriga, K. Franze, G. Charras, and R. Mayor, "Tissue Stiffening Coordinates Morphogenesis by Triggering Collective Cell Migration in Vivo," *Nature* 554, no. 7693 (2018): 523–527.

14. L. Scaccini, A. Battisti, D. Convertino, et al., "Glycerol-Blended Chitosan Membranes With Directional Micro-Grooves and Reduced Stiffness Improve Schwann Cell Wound Healing," *Biomedical Materials* 19, no. 6 (2024): 065005.

15. A. M. Hopkins, E. DeSimone, K. Chwalek, and D. L. Kaplan, "3D in Vitro Modeling of the Central Nervous System," *Progress in Neurobiology* 125 (2015): 1–25.

16. B. Qiu, N. Bessler, K. Figler, et al., "Bioprinting Neural Systems to Model Central Nervous System Diseases," *Advanced Functional Materials* 30, no. 44 (2020): 1910250.

17. S. Neziri, A. E. Köseoğlu, G. Deniz Köseoğlu, B. Özgültekin, and N. Ö. Özgentürk, "Animal Models in Neuroscience With Alternative Approaches: Evolutionary, Biomedical, and Ethical Perspectives," *Animal Models and Experimental Medicine* 7, no. 6 (2024): 868–880.

18. A. Vashishat, P. Patel, G. das Gupta, and B. das Kurmi, "Alternatives of Animal Models for Biomedical Research: A Comprehensive Review of Modern Approaches," *Stem Cell Reviews and Reports* 20, no. 4 (2024): 881–899.

19. E. Redolfi Riva, M. Özkan, E. Contreras, et al., "Beyond the Limiting Gap Length: Peripheral Nerve Regeneration Through Implantable Nerve Guidance Conduits," *Biomaterials Science* 12, no. 6 (2024): 1371–1404.

20. A. Malheiro, P. Wieringa, and L. Moroni, "Peripheral Neurovascular Link: An Overview of Interactions and In Vitro Models," *Trends in Endocrinology and Metabolism* 32, no. 8 (2021): 623–638.

21. J. M. Grasman, J. A. Ferreira, and D. L. Kaplan, "Tissue Models for Neurogenesis and Repair in 3D," *Advanced Functional Materials* 28, no. 48 (2018): 1–10.

22. D. Kraus, V. Boyle, N. Leibig, G. B. Stark, and V. Penna, "The Neuro-Spheroid-A Novel 3D In Vitro Model for Peripheral Nerve Regeneration," *Journal of Neuroscience Methods* 246 (2015): 97–105.

23. Y.-J. Lin, Y. W. Lee, C. W. Chang, and C. C. Huang, "3D Spheroids of Umbilical Cord Blood MSC-Derived Schwann Cells Promote Peripheral Nerve Regeneration," *Frontiers in Cell and Developmental Biology* 8 (2020): 604946.

24. M. F. Daud, M. F. B. Daud, K. C. Pawar, F. Claeyssens, A. J. Ryan, and J. W. Haycock, "An Aligned 3D Neuronal-Glial Co-Culture Model for Peripheral Nerve Studies," *Biomaterials* 33, no. 25 (2012): 5901–5913.

25. A. Malheiro, A. Harichandan, J. Bernardi, et al., "3D Culture Platform of Human iPSCs-Derived Nociceptors for Peripheral Nerve Modeling and Tissue Innervation," *Biofabrication* 14, no. 1 (2021): 1–21.

26. S. Geuna, S. Raimondo, F. Fregnan, K. Haastert-Talini, and C. Grothe, "In Vitro Models for Peripheral Nerve Regeneration," *European Journal of Neuroscience* 43, no. 3 (2016): 287–296.

27. M. Fornaro, A. Giovannelli, A. Foggetti, et al., "Role of Neurotrophic Factors in Enhancing Linear Axonal Growth of Ganglionic Sensory Neurons in Vitro," *Neural Regeneration Research* 15, no. 9 (2020): 1732–1739.

28. F. Fregnan, L. Muratori, A. Crosio, et al., "A Novel Rat Model for Studying Bilateral Cavernous Nerve Damage in Vivo: Exploring the Potential of Chitosan-Blended Membranes for Nerve Regeneration Post-Radical Prostatectomy," *Minerva Urology and Nephrology* 77, no. 1 (2025): 91–110.

29. S. Fueshko and S. Wray, "LHRH Cells Migrate on Peripherin Fibers in Embryonic Olfactory Explant Cultures: An in Vitro Model for Neurophilic Neuronal Migration," *Developmental Biology* 166, no. 1 (1994): 331–348.

30. A. Malheiro, F. Morgan, M. Baker, L. Moroni, and P. Wieringa, "A Three-Dimensional Biomimetic Peripheral Nerve Model for Drug Testing and Disease Modelling," *Biomaterials* 257 (2020): 120230.

31. R. Kaewkhaw, A. M. Scutt, and J. W. Haycock, "Integrated Culture and Purification of Rat Schwann Cells From Freshly Isolated Adult Tissue," *Nature Protocols* 7, no. 11 (2012): 1996–2004.

32. I. Tonazzini, C. Masciullo, E. Savi, A. Sonato, F. Romanato, and M. Cecchini, "Neuronal Contact Guidance and YAP Signaling on Ultra-Small Nanogratings," *Scientific Reports* 10, no. 1 (2020): 3742.

33. G. Rosso and J. Guck, "Mechanical Changes of Peripheral Nerve Tissue Microenvironment and Their Structural Basis During Development," *APL Bioengineering* 3, no. 3 (2019): 036107.

34. K. R. Moss, R. Mi, R. Kawaguchi, et al., "hESC- and hiPSC-Derived Schwann Cells Are Molecularly Comparable and Functionally Equivalent," *iScience* 27, no. 6 (2024): 109855.

35. K. R. Jessen and R. Mirsky, "The Repair Schwann Cell and Its Function in Regenerating Nerves," *Journal of Physiology* 594, no. 13 (2016): 3521–3531.

36. K. V. Panzer, J. C. Burrell, K. V. T. Helm, et al., "Tissue Engineered Bands of Büngner for Accelerated Motor and Sensory Axonal Outgrowth," *Frontiers in Bioengineering and Biotechnology* 8 (2020): 580654.

37. B. E. Fornasari, F. Zen, G. Nato, et al., "Blood Vessels: The Pathway Used by Schwann Cells to Colonize Nerve Conduits," *International Journal of Molecular Sciences* 23, no. 4 (2022): 2254.

38. M. Georgiou, S. C. Bunting, H. A. Davies, A. J. Loughlin, J. P. Golding, and J. B. Phillips, "Engineered Neural Tissue for Peripheral Nerve Repair," *Biomaterials* 34, no. 30 (2013): 7335–7343.